Hindawi
Advances in OptoElectronics
Volume 2018, Article ID 7368175, 5 pages
https://doi.org/10.1155/2018/7368175

Research Article

HIT Solar Cells with N-Type Low-Cost Metallurgical Si

Xing Yang,[1] Jiangtao Bian,[2] Zhengxin Liu,[2] Shuai Li,[1] Chao Chen,[1] and Song He[1]

[1]*College of Energy, Xiamen University, Xiamen, China*
[2]*Shanghai Institute of Micro-System and Information Technology, Chinese Academy of Sciences, Shanghai, China*

Correspondence should be addressed to Chao Chen; cchen@xmu.edu.cn and Song He; hes@xmu.edu.cn

Received 20 August 2017; Revised 23 November 2017; Accepted 17 December 2017; Published 18 January 2018

Academic Editor: Jung Y. Huang

A conversion efficiency of 20.23% of heterojunction with intrinsic thin layer (HIT) solar cell on 156 mm × 156 mm metallurgical Si wafer has been obtained. Applying AFORS-HET software simulation, HIT solar cell with metallurgical Si was investigated with regard to impurity concentration, compensation level, and their impacts on cell performance. It is known that a small amount of impurity in metallurgical Si materials is not harmful to solar cell properties.

1. Introduction

It is always the ultimate goal for PV industry to achieve both high conversion efficiency and low cost. Heterojunction with intrinsic thin layer (HIT) solar cells realizes high open-circuit voltage and hence high conversion efficiency by applying hydrogen-rich a-Si passivation to N-type Si wafer. Panasonic (formerly Sanyo) realized the highest HIT conversion efficiency of 25.6% [1]. However, the high manufacturing cost (~$0.5/w) of HIT solar cell becomes the main obstacle for further capacity expansion. Currently, solar-grade Si (SOG-Si) is mainly fabricated using improved Siemens method. However, such method faces high energy consumption, high cost, and pollution issues. Si purification using metallurgical method has drawn attention for the past ten years due to its low cost, low energy consumption, and less pollution. N-type Si using metallurgical method does not require the expensive e-beam phosphorus removal process step, and therefore its manufacturing cost is only 40% compared to Siemens method. An et al. [2] investigated the main solar cell performance for both Siemens and metallurgical methods and obtained the conversion efficiency for regular monocrystalline metallurgical Si to be 18.3%. More attention should be paid to the Einhaus research group [3], a cell efficiency of 19% for mono-c UMG N-type Si has been demonstrated on a 149 cm^2 cell in first trials using heterojunction solar cell technology. AFORS-HET (Automat for Simulation of Heterostructures) was developed specifically for heterojunction solar cell, which can simulate any type of semiconductor tandem materials with random combination. Researchers investigated HIT solar cell performance using AFORS-HET simulation and obtained valuable results [4–6]. In this study, AFORS-HET simulation was applied to investigate the HIT solar cell with metallurgical Si. HIT solar cells with both Siemens and metallurgical Si were fabricated for comparison purposes.

2. HIT Solar Cell Fabrication

HIT solar cells using both Siemens and metallurgical N-type Si wafers (156 × 156 mm^2) were fabricated using ULVAC plasma enhanced chemical vapor deposition (PECVD) for 5~10 nm a-Si films and Sumitomo reactive plasma deposition (RPD) for transparent conductive oxide (TCO) preparation. Finally, screen printing was applied to form silver metal contact to extract the light-generated current. The HIT solar cells were fabricated with four-bus-bar design and bifacial structure (Figure 1(a)). The processing temperature for the whole HIT solar cell processing is less than 250°C. *I-V* parameters were characterized with a Kopel steady-state IV tester.

3. AFORS-HET Simulation

Si materials produced by metallurgical method have the following properties: (1) impurity compensation phenomenon,

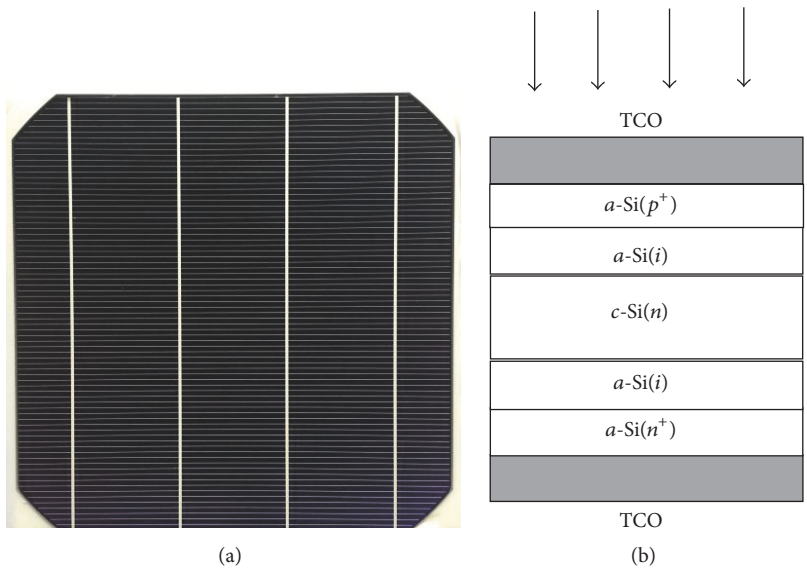

Figure 1: (a) Front side fabricated HIT solar cell. (b) Schematic diagram of HIT solar cell structure.

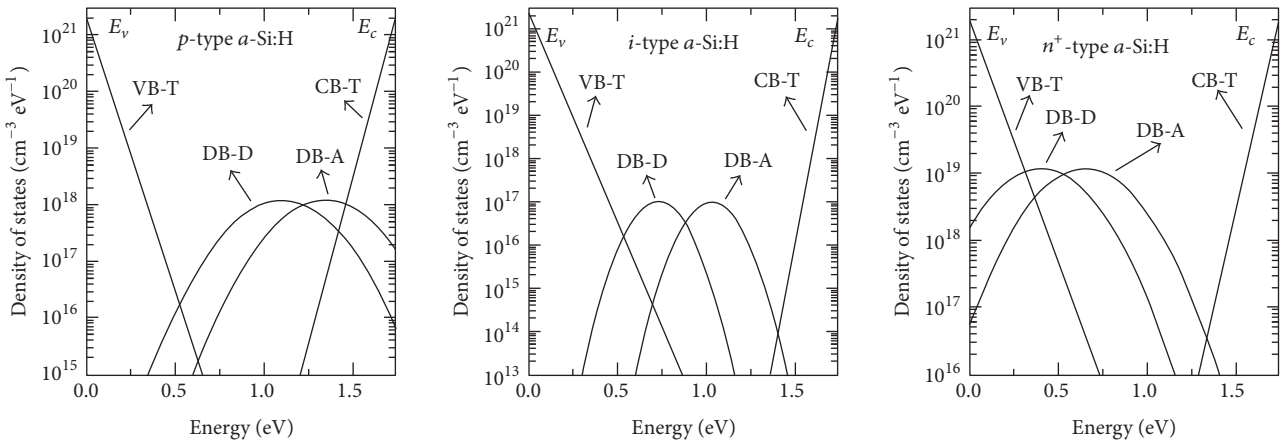

Figure 2: Defect state distributions of different types of a-Si:H in the simulations.

for example, coexistence of boron and phosphorus and (2) higher concentration level of metal impurities, for example, iron (Fe) and copper (Cu). It is well known that Fe and Cu concentrations in Si by Siemens method are negligible. The metallurgical Si wafers used in this work had resistivity of 2.0 Ω·cm, minority carrier lifetime of 30 μs, and Fe concentration of 0.005 ppb. The tested parameters of Si wafers were input into AFORS-HET software for the simulated analysis of HIT solar cell, investigating the impact of metal impurity and boron and phosphorus compensation on the cell properties. In AFORS-HET, the doping concentration can be both boron and phosphorus, and the impurity level can be easily adjusted, which is suitable for compensated HIT solar cell research. The HIT solar cell structure for this simulation is p^+-a-Si/i-a-Si:H/c-Si/i-a-Si:H/n^+-a-Si (Figure 1(b)). The parameters for the simulation are obtained from other publications [7–10] and listed in Table 1. The Si substrate used in this simulation was 170 μm which is smaller than 190 μm of bare Si wafer due to the thickness reduction by acid etching. The surface recombination at the a-Si/c-Si interface is 1.0×10^7 cms^{-1}. The defect state [6] setting for p^+-a-Si, i-a-Si, and n^+-a-Si is shown in Figure 2. Light trapping is added on both front and back surfaces. Both front and back electrodes are in Ohmic contact. The reflectivity for front and back surfaces is 0.1 and 1, respectively. The simulated light soaking condition is AM1.5, 100 mW/cm^2. The effective wavelength region is 0.38~1.1 μm.

4. Results and Discussion

4.1. The Influence of Deep Energy-Level Impurity on the Solar Cell Properties. Si purification by metallurgical method can be realized through gas blowing, slagging boron removal, electron beam refining phosphorus removal, acid leaching, and unidirectional solidification metals removal. The repeated processes were applied to remove the metal impurities in Si and reach SOG requirements. However, the

Table 1: Input parameters for AFORS-HET simulation.

Parameters	a-Si:H(p)	a-Si:H(i)	c-Si(n)	a-Si:H(n^+)
Thickness (nm)	5	5	1.7×10^5	5
Dielectric constant	11.9	11.9	11.9	11.9
Electron affinity (eV)	3.8	3.8	4.05	3.8
Band gap (eV)	1.70	1.74	1.12	1.70
Effective conduction band density (cm^{-3})	1.0×10^{20}	1.0×10^{20}	2.8×10^{19}	1.0×10^{20}
Effective valence band density (cm^{-3})	1.0×10^{20}	1.0×10^{20}	1.04×10^{19}	1.0×10^{20}
Electron mobility ($cm^2V^{-1}s^{-1}$)	10	20	1040	10
Hole mobility ($cm^2V^{-1}s^{-1}$)	1	2	412	1
Acceptor concentration (cm^{-3})	1.0×10^{19}	0	5×10^{15}	0
Donor concentration (cm^{-3})	0	0	7.03×10^{15}	1.0×10^{19}
Thermal velocity of electrons (cm/s)	1.0×10^7	1.0×10^7	1.0×10^7	1.0×10^7
Thermal velocity of hole (cm/s)	1.0×10^7	1.0×10^7	1.0×10^7	1.0×10^7
Layer density ($g * cm^{-3}$)	2.328	2.328	2.328	2.328
Band tail density of states ($cm^{-3}eV^{-1}$)	2.0×10^{21}	2.0×10^{21}		2.0×10^{21}
Characteristic energy (eV) for donors, acceptors	0.045, 0.037	0.045, 0.02		0.06, 0.037
Capture cross-section for donor states, e, h (cm^2)	1.0×10^{-15}, 1.0×10^{-17}	1.0×10^{-15}, 1.0×10^{-17}		1.0×10^{-15}, 1.0×10^{-17}
Capture cross-section for acceptor states, e, h (cm^2)	1.0×10^{-17}, 1.0×10^{-15}	1.0×10^{-17}, 1.0×10^{-15}		1.0×10^{-17}, 1.0×10^{-15}
defect density of states at Gaussian peak energy (eV)	1.0×10^{17}~6.0×10^{19}	1.0×10^{16}~1.0×10^{19}		8.0×10^{17}~1.0×10^{20}
Standard deviation (eV)	1.10, 1.35	0.725, 1.025		0.40, 0.65
Capture cross-section for donor states, e, h (cm^2)	1.0×10^{-14}, 1.0×10^{-15}	1.0×10^{-14}, 1.0×10^{-15}		1.0×10^{-14}, 1.0×10^{-15}
Capture cross-section for acceptor states, e, h (cm^2)	1.0×10^{-15}, 1.0×10^{-14}	1.0×10^{-15}, 1.0×10^{-14}		1.0×10^{-15}, 1.0×10^{-14}

metal impurities in Si with Siemens method are higher. The metal impurities (Fe, Cu, and Ni) lead to a decrease of minority carrier lifetime, reducing the light-generated current. In AFORS-HET, defects can be deliberately added to c-Si for simulating the impact of metal impurities on solar cell properties. In this work, only Fe and Cu are considered to be the two main metal impurities. Due to the directional solidification of Fe residue, electron beam processing with copper electrodes may be introduced. The energy levels of Fe and Cu in Si are 0.4 eV and 0.24 eV, respectively. The electron capture cross-sections for Fe and Cu are 4.5×10^{-14} cm^{-2} and 1×10^{-14} cm^{-2}, respectively [10]. The hole capture cross-sections for Fe and Cu are 6.91×10^{-17} cm^{-2} and 1.8×10^{-17} cm^{-2}, respectively. First, we only consider Fe impurity and set the concentration range to be 1×10^{10} cm^{-3} ~1×10^{15} cm^{-3}. The solar cell properties are shown in Figure 3(a). From Figure 3(a), the results indicate that the density of defect states should be less than 10^{12} cm^{-3} in order to obtain a good performance. However, when Dit > 10^{12} cm^{-3}, cell properties are seriously affected by defect state. The conversion efficiency drops below 20%. Meanwhile, short-circuit current density (J_{sc}) and open-circuit voltage (V_{oc}) both decrease. When Fe impurity concentration level increases up to 10^{15} cm^{-3}, V_{oc} decreases to 468 mv and J_{sc} drops to 24.21 mA/cm^2. The conversion efficiency is only 8.07%. Figure 3(b) shows the simulation results when both Fe and Cu impurities exist. During the simulation, Fe impurity level was fixed to be 10^{12} cm^{-3}, while the concentration of Cu impurity varied within 1×10^{10} cm^{-3}~1×10^{15} cm^{-3}. From the simulation results, we can see that when Cu concentration is over 10^{12} cm^{-3}, the conversion efficiency (η) decreases less than 20%. The cell performance gets worse with the increase of Cu impurity concentration. In combination with the data from Figures 3(a) and 3(b), it can be seen that the effects of multiple impurities are added to each other. The main impurities in metallurgical Si material are Fe and Cu. The measured Fe and Cu concentrations are 2.6×10^{12} cm^{-3} and 6.5×10^{11} cm^{-3} by glow discharge mass spectrometry (GDMS), respectively. Inputting the measured impurity data into AFORS-HET software, we obtained the simulated V_{oc} ~ 684.1 mV, J_{sc} ~ 39.89 mA/cm^2, fill factor (FF) ~ 75.08%, and η ~ 19.58%.

4.2. Influence of Compensation Level on Solar Cell Properties. In metallurgical N-type Si wafer, there are certain amounts of boron doping besides phosphorus, which is a well-known compensation phenomenon, and the compensation is proportional to the concentration of boron. In AFORS-HET simulation, donor concentration N_D and acceptor concentration N_A can be input simultaneously. The carrier mobility is input manually as a fixed parameter, as carrier mobility at different doping concentrations is different. At room temperature, carrier mobility in Si can be presented with the following equation [11]:

$$\mu_n = \frac{5.096 \times 10^{18} + 92 \times N_A^{0.91}}{3.747 \times 10^{15} + N_A^{0.91}},$$
$$\mu_p = \frac{2.898 \times 10^{15} + 4.77 \times N_D^{0.76}}{5.855 \times 10^{12} + N_D^{0.76}}. \quad (1)$$

Equations (1) reflect the concentration of donor or acceptor impurities at room temperature. For a more accurate

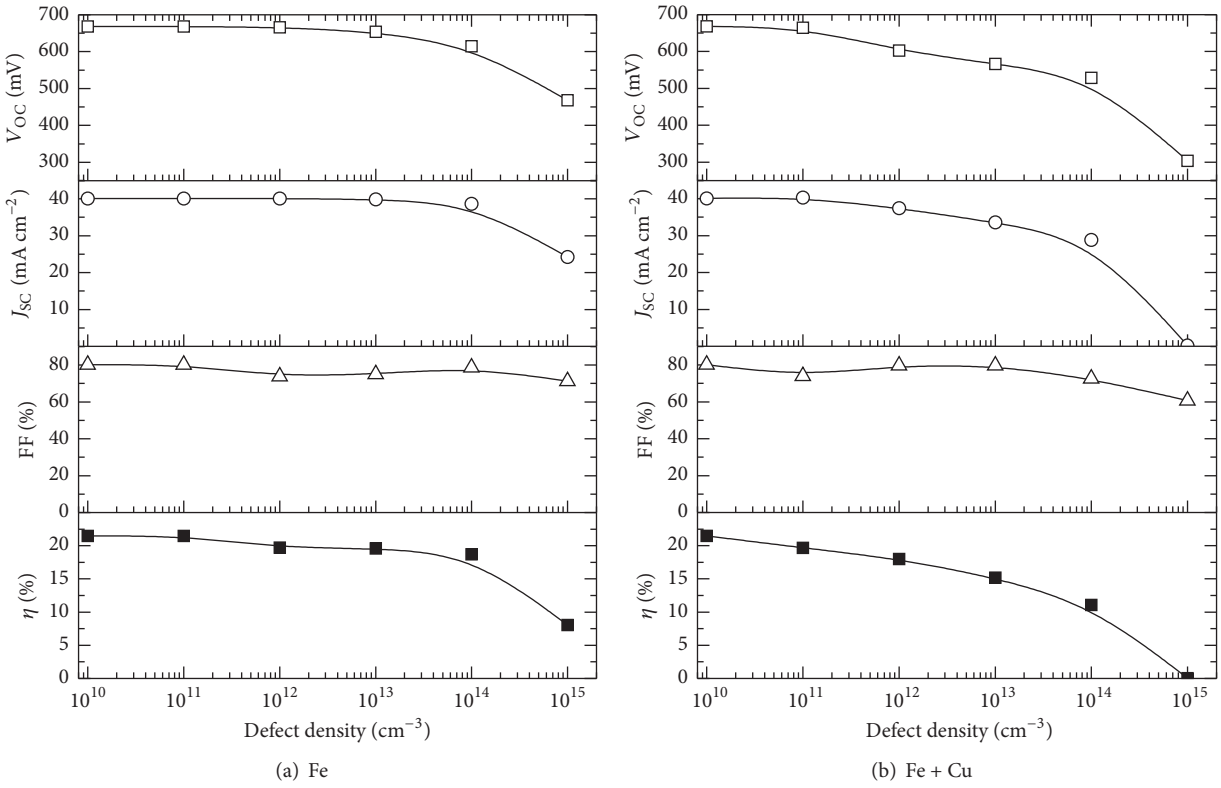

Figure 3: (a) Impact of Fe impurity on cell properties. (b) Impact of Fe + Cu on cell properties.

simulation of the compensation influence on cell properties, the differences between N_D and N_A are calculated and set to be 2.03×10^{15} cm^{-3}. The acceptor concentration N_A varies within 1×10^{15} cm^{-3}~2×10^{16} cm^{-3}. Electron mobility and hole mobility are calculated with MATLAB software and input into AFORS-HET for simulation. The simulated results are shown in Figure 4. It can be seen from Figure 4 that the influence of compensation on cell properties is minor. The more the compensation is, the worse the cell properties are. The measured N_A for metallurgical Si is 1.368×10^{15} cm^{-3} by GDMS.

4.3. Comparison of Simulated and Measured Solar Cell Properties. In this work, the metallurgical Si wafers were used to fabricate 156 mm × 156 mm HIT solar cells in a pilot line at Shanghai Institute of Micro-System and Information Technology, Chinese Academy of Sciences. The same fabrication processes were used to prepare the same batch of Siemens Si HIT cell for contrast. The *I-V* curves of both types of HIT solar cells using metallurgical Si and Siemens Si were shown in Figure 5.

The measured parameters for metallurgical Si were introduced into AFORS-HET software for simulation of HIT solar cell. Table 2 shows the simulated and measured cell properties for comparison. It can be seen that V_{oc}, J_{sc}, FF, and η for both simulated and measured HIT solar cells are similar. However, the temperature coefficient (TC) of photoelectric conversion efficiency for simulated sample is smaller than that of the measured data. With AFORS-HET software optimization, HIT solar cell with metallurgical Si can reach up to 21.17%, when density of defect states is 10^{12} cm^{-3} and the concentration of boron is zero. Table 2 also shows the cell performance comparison for one metallurgical Si sample and one Siemens Si sample from the same batches. The electrical properties of the metallurgical Si samples are slightly worse than those of Siemens Si sample. Considering the significantly low cost of metallurgical Si materials, the performance to cost ratio for metallurgical Si HIT solar cells would be higher than that of Siemens Si solar cell, meaning that the metallurgical Si HIT solar cells have a great potential for industrial large-scale manufacturing.

5. Conclusions

It can be concluded that although the material quality of metallurgical Si is relatively worse than that of Siemens method, HIT solar cells with competitive performance can still be achieved. The best performance of metallurgical HIT solar cell is $V_{oc} \sim 694.9$ mV, $J_{sc} \sim 37.564$ mA/cm^2, FF ~ 77.48%, $\eta \sim 20.23\%$, and TC ~ −0.3043%/°C. From the analysis based on AFORS-HET software simulation, it is known that a small amount of impurity in metallurgical Si materials is not harmful to solar cell properties.

Conflicts of Interest

The authors declare no conflicts of interest regarding the publication of this paper.

Table 2: Comparison of HIT solar cell properties with metallurgical and Siemens Si samples.

Cell parameters	Siemens Si	Metallurgical Si	Simulated data	Optimized data
V_{oc} (V)	0.7294	0.6949	0.6841	0.7061
J_{sc} (mA/cm^2)	38.918	37.564	37.656	39.641
FF (%)	78.37	77.48	75.08	81.08
η (%)	22.25	20.23	19.58	21.17
TC (%/°C)	−0.225	−0.3043	−0.2000	−0.2000

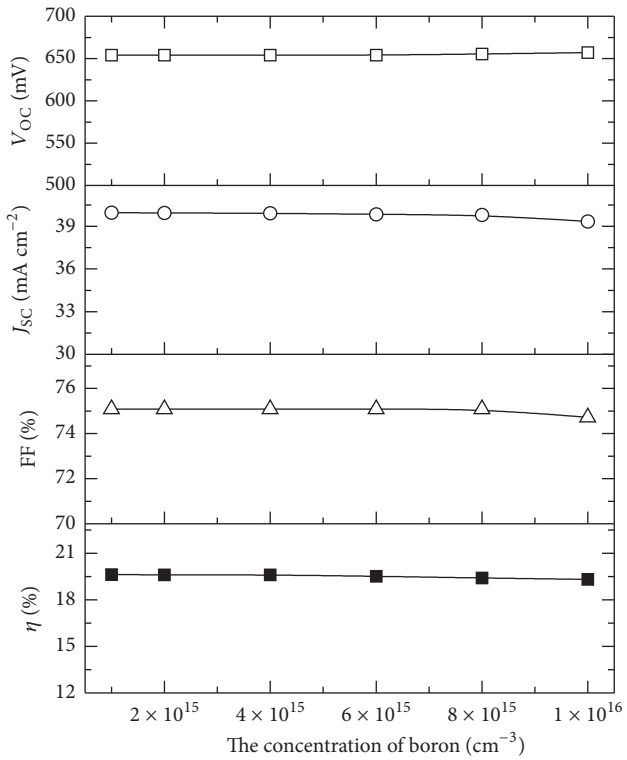

Figure 4: Influence of compensation level on solar cell properties.

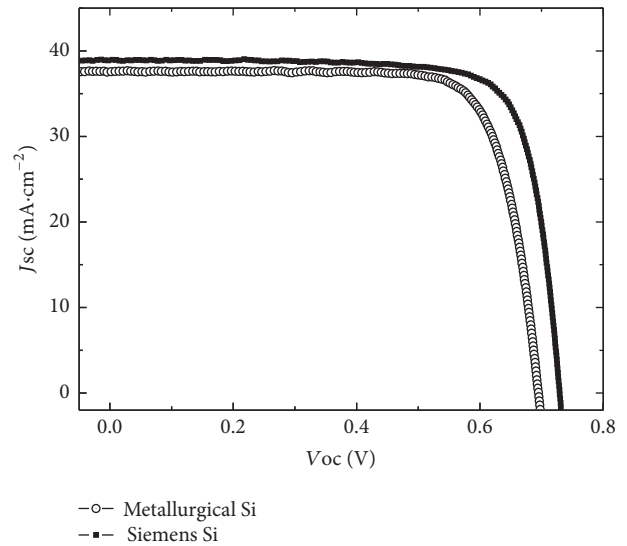

Figure 5: Comparison of *I-V* curves of HIT cells using metallurgical Si and Siemens Si.

Acknowledgments

The authors appreciate the financial sponsorship from Fujian Industrial Guidance Project (no. 2017H0038). Also thanks are given to Ningxia Power Group Co., Ltd., China, for providing N-type monocrystalline SOG silicon rods purified with metallurgical method.

References

[1] K. Masuko, M. Shigematsu, T. Hashiguchi et al., "Achievement of more than 25% conversion efficiency with crystalline silicon heterojunction solar cell," *IEEE Journal of Photovoltaics*, vol. 4, no. 6, pp. 1433–1435, 2014.

[2] B. An J, J. Yank, and X. Zhou, "Electrical performance comparison of mono-crystalline silicon solar cell with wafer purified by metallurgical Siemens method," *ActaEnergiae Solaris Sinica*, vol. 36, pp. 2325–2328, 2015.

[3] R. Einhaus, J. Kraiem, J. Degoulange et al., "19% efficiency heterojunction solar cells on Cz wafers from non-blended Upgraded Metallurgical Silicon," in *Proceedings of the 2012 IEEE 38th Photovoltaic Specialists Conference (PVSC)*, pp. 003234–003237, Austin, TX, USA, June 2012.

[4] B. Ren, Y. Zhang, B. Guo et al., "Computer simulation of a-si:H/c-Si heterjuntion solar cells on n-type silicon," *ActaEnergiae Solaris Sinica*, vol. 29, pp. 1112–1116, 2008.

[5] X. Cheng, F. Meng, J. Wang, X. Li, and J. Huang, "Simulation of heterojunction solar cells based on p-type silicon wafer," *Acta Energiae Solaris Sinica*, vol. 33, no. 9, pp. 1474–1479, 2012.

[6] X. Wen, X. Zeng, W. Liao, Q. Lei, and S. Yin, "An approach for improving the carriers transport properties of a-Si: H/c-Si heterojunction solar cells with efficiency of more than 27%," *Solar Energy*, vol. 96, pp. 168–176, 2013.

[7] K. Patel, M. Katiyar, B. Mazhari et al., "Simulation studies on heterojunction and HIT solar cells," in *Proceedings of the 16th International Workshop on Physics of Semiconductor Devices*, p. 85490E, Kanpur, India.

[8] J. Liu, S. Huang, and L. He, "Simulation of a high-efficiency silicon-based heterojunction solar cell," *Journal of Semiconductors*, vol. 36, no. 4, pp. 0440101–0440108, 2015.

[9] N. Dwivedi, S. Kumar, A. Bisht, K. Patel, and S. Sudhakar, "Simulation approach for optimization of device structure and thickness of HIT solar cells to achieve ~27% efficiency," *Solar Energy*, vol. 88, pp. 31–41, 2013.

[10] L. Zhao, H. L. Li, C. L. Zhou, H. W. Diao, and W. J. Wang, "Optimized resistivity of p-type Si substrate for HIT solar cell with Al back surface field by computer simulation," *Solar Energy*, vol. 83, no. 6, pp. 812–816, 2009.

[11] Z. Chen and J. Wang, *Basic Material Physics for Semiconductor Devices*, Science Press, 2013.